Nuclear Physics B87 (1975) 461–479

ELECTRON-POSITRON ANNIHILATION INTO PIONS IN AN ANALYTIC MODEL OF CURRENT-HADRONIC INTERACTIONS *

J.W. MOFFAT, P. SAVARIA and A.C.D. WRIGHT **
Department of Physics, University of Toronto, Toronto, Canada

Received 11 June 1974
(Revised 22 October 1974)

We present an analytic model for virtual pion Compton scattering. Using factorization of the Regge residues we predict the scale-invariant electroproduction structure functions for $e^- \pi \to e^- X$, and obtain results for the pion form factor that compare well with the data. By fitting recent data from CEA and the SLAC-LBL-SPEAR collaboration for the ratio $R = \sigma(e^+e^- \to \text{hadrons})/\sigma(e^+e^- \to \mu^+\mu^-)$, and for the mean multiplicity of charged pions, we obtain predictions for the inclusive process $e^+e^- \to \pi^- X$. In particular, the predicted $E_\pi d^3\sigma/dp^3$ for the inclusive process $e^+e^- \to \pi^- X$ shows a strong diffractive type of behaviour with a slope for $\sqrt{q^2} \sim 4.8$ GeV approximately the same as in $pp \to \pi^- X$. The ratio R is predicted to rise linearly *versus* $\sqrt{q^2}$ until some high energy, beyond which it tends to a constant, while the multiplicity remains essentially constant. The mechanism in the model that produces these predictions is the build-up or "statistical bootstrapping" of meson resonances in the direct (or missing mass) s-channel.

1. Introduction

Recent experiments [1, 2] have revealed that up to a total c.m. energy of 5 GeV, the total cross section for the process $e^+ + e^- \to$ hadrons may be falling more slowly with increasing energy than $\sigma_{\mu^+\mu^-}$, the point-like cross section for $e^+ + e^- \to \mu^+ + \mu^-$. This behaviour is already in conflict with the generalized vector dominance model [3], which predicts that $R(q^2) \equiv \sigma_{\text{tot}}(q^2)/\sigma_{\mu^+\mu^-}(q^2) \sim$ const. for moderate values of q^2, as is required to explain the early onset of scale invariance of the nucleon electroproduction structure function.

Furthermore, the new data have inspired a reexamination of the parton (or quark) models [4] which, in their simplest forms, predict that $R(q^2) \sim$ const. for asymptotic values of q^2. It has been suggested [5] that the annihilation data have not yet reached their scale-invariant limit, so that the simple parton model is not

* Supported in part by the National Research Council of Canada.
** Present address: Stanford Linear Accelerator Center, Stanford University, Stanford, California, 94305, USA.

valid at $q^2 = 25$ GeV^2, and requires modification for finite q^2. Of course, we are still left with the fundamental question of why the quarks or partons have not yet been observed.

In this paper, we study electron-positron annihilation into pions by extending a model for the nucleon Compton amplitude [6] to the case of pion Compton scattering. The model satisfies the following fundamental requirements: (a) Mandelstam analyticity, (b) crossing symmetry, (c) scale invariance in the limit $|q^2| \to \infty$, (d) Regge behaviour in all channels, (e) resonance poles in the unphysical sheet, (f) generalized vector meson dominance (i.e. the model contains cuts in q^2 as well as poles in the second sheet of the q^2 plane), (g) SU(3) structure of the currents.

In sect. 2, crossing symmetry and isospin invariance are used to obtain the form of the amplitude, and a model analogous to the nucleon Compton amplitude in ref. [6] is obtained. The analytically continued form of the amplitude is derived in the annihilation region. We implement factorization of the pomeron and P$'$ residues in the Regge limit in sect. 3. By requiring that the threshold behaviour of the scale-invariant electroproduction structure function be smooth in our model, a prediction is obtained for the structure function. The pion form factor is then predicted with the help of the Bloom-Gilman sum rule [7–8] and compared with recent data. In sect. 4, we formulate inclusive sum rules to obtain the total cross section and mean multiplicity of pions produced in e^+e^- annihilation in terms of the cross section for $e^+ + e^- \to \pi + X$. In sect. 5, we discuss the results obtained from fitting the total cross section and mean multiplicity. With the scale invariance breaking behaviour of the model thus determined, we are able to make predictions for the annihilation structure function, and the inclusive pion production cross sections for finite values of q^2. In sect. 6, we end with some concluding remarks about our results.

2. Analytic model

Following ref. [6], we define the double helicity-flip amplitude for pion Compton scattering by

$$T_2^\pi(s, t, q_1^2, q_2^2) = -(q_1 \cdot q_2)A(s, t, q_1^2, q_2^2) + B(s, t, q_1^2, q_2^2)\,, \tag{2.1}$$

where we assume that A satisfies a Mandelstam representation and B is the Born term. The amplitude A can be written as a sum of contributions from isovector ($i = 3$) and isoscalar ($i = 8$) photons

$$A = A_{33} + \frac{1}{\sqrt{3}}A_{38} + \frac{1}{\sqrt{3}}A_{83} + \tfrac{1}{3}A_{88}\,. \tag{2.2}$$

The amplitudes A_{ij} may be decomposed into amplitudes of definite isospin I, denoted by A_{ij}^I. We write

$$A^I_{ij} = F^I_{ij} + P^I_{ij}\,, \tag{2.3}$$

where F is the non-diffractive contribution and P is the pomeron contribution.

For the isovector-isovector amplitude A_{33}, we require that the exotic $I = 2$ amplitudes must contain no s, t and u poles in the s, t and u channels, respectively. For example, in the s-channel:

$$F^2_{33}(s,t,u) = F^{33}(u,t)\,. \tag{2.4}$$

This function $F^{33}(x,y)$ has poles in both x and y, but is not symmetric in these variables. Thus $F^{33}(s,t)$ has resonances lying on the exchange-degenerate $\rho-\mathrm{P}'-\mathrm{A}_2-\omega$ trajectory in the s- and t-channels (we have omitted q_1^2 and q_2^2 for convenience). We further require that no pole occur more than once in the amplitudes. To satisfy these assumptions and s–u crossing symmetry we are led, using crossing relations, to the following form:

$$F^1_{33}(s,t,u) = F^{33}(s,t)\,, \tag{2.5}$$

$$F^0_{33}(s,t,u) = -\tfrac{1}{2}F^{33}(u,t) + \tfrac{3}{2}F^{33}(s,t)\,. \tag{2.6}$$

To discuss the pomeron amplitude, we introduce the function $A_{\mathrm{P}}(t,s)$ which has a pomeron exchanged in the t-channel and no s-channel resonances. By requiring that the pomeron be exchanged only in the t-channel and that the Pomeranchuk theorem be satisfied, we obtain

$$P^2_{33}(s,t,u) = P^1_{33}(s,t,u) = P^0_{33}(s,t,u) = A^{33}_{\mathrm{P}}(t,s) + A^{33}_{\mathrm{P}}(t,u)\,. \tag{2.7}$$

For A_{88}, we have that

$$F^1_{88}(s,t,u) = F^{88}(s,t) + F^{88}(u,t)\,, \tag{2.8}$$

$$P^1_{88}(s,t,u) = A^{88}_{\mathrm{P}}(t,s) + A^{88}_{\mathrm{P}}(t,u)\,. \tag{2.9}$$

Neither the pomeron nor any of the leading non-diffractive t-channel exchanges can contribute to the amplitudes A_{38} and A_{83}. Although the s-channel exchanges cannot be ruled out so easily, we have investigated the effects of "non-diagonal" terms, such as A_{38}, and find that their inclusion does not alter our results.

The various pion Compton amplitudes are now given by

$$\begin{aligned} A(\pi^\pm\gamma \to \pi^\pm\gamma) &= \tfrac{1}{2}(A^1_{33}+A^2_{33}) + \tfrac{1}{3}A^1_{88} \\ &= \tfrac{1}{2}(F^{33}(s,t)+F^{33}(u,t)) + A^{33}_{\mathrm{P}}(t,s) + A^{33}_{\mathrm{P}}(t,u) \\ &\quad + \tfrac{1}{3}(F^{88}(s,t)+F^{88}(u,t)+A^{88}_{\mathrm{P}}(t,s)+A^{88}_{\mathrm{P}}(t,u))\,, \end{aligned} \tag{2.10}$$

$$A(\pi^0\gamma \to \pi^0\gamma) = \tfrac{1}{3}A^0_{33} + \tfrac{2}{3}A^2_{33} + \tfrac{1}{3}A^1_{88}$$
$$= A(\pi^\pm\gamma \to \pi^\pm\gamma)\,.$$

The construction of the pomeron and non-diffractive amplitudes is analogous to the nucleon-photon case, discussed in ref. [6]. We have

$$A^{ii}_{\mathrm{P}}(t, s, q_1^2, q_2^2) = \gamma^{ii}_{\mathrm{P}}(t) \ln [1 + (1-\omega')^{\frac{1}{2}}]$$
$$\times\, w_{\mathrm{P}}(\omega')^{\alpha_{\mathrm{P}}(t)-2}\, \mathcal{F}(q_1^2, q_2^2) D_i(q_1^2) D_i(q_2^2)\,, \qquad (i = 3, 8)\,, \tag{2.12}$$

$$F^{ii}(s, t, q_1^2, q_2^2) = -[\gamma^{ii}(\omega')\Gamma(1-\alpha_\rho(s)) w_\rho(t)^{\alpha_\rho(s)}$$
$$+ \gamma^{ii}_{\mathrm{P}'}(t)\Gamma(2-\alpha_\rho(t)) w_{\mathrm{P}'}(\omega')^{\alpha_\rho(t)-2}\, \mathcal{F}(q_1^2, q_2^2)]$$
$$\times\, D_i(q_1^2) D_i(q_2^2) + \Sigma(\text{satellites})\,, \qquad (i = 3, 8)\,. \tag{2.13}$$

Here, the variable ω' is defined by

$$\omega' = 1 + x_1 x_2 (s - s_t)\,, \tag{2.14}$$

where

$$x_i = [a + (q_t^2 - q_i^2)^{\frac{1}{2}}]^{-1}\,, \qquad (i = 1, 2)\,. \tag{2.15}$$

The elastic threshold is given by

$$s_t = 4m_\pi^2\,, \tag{2.16}$$

whereas q_t and a are given by

$$q_t = 0.99\ \mathrm{GeV}/c\,, \qquad a = 0.12\ \mathrm{GeV}/c\,. \tag{2.17}$$

The vector meson propagators $D_3(q^2)$ and $D_8(q^2)$ are the same as in ref. [6], and the $\mathcal{F}$ function is given by

$$\mathcal{F}(q_1^2, q_2^2) = 1 + f(q_1^2) f(q_2^2)\,, \tag{2.18}$$

where

$$f(q^2) = \frac{cq^2(m_\omega^2 - q^2)}{[a + (q_t^2 - q^2)^{\frac{1}{2}}]^n}\,, \tag{2.19}$$

with $c = 4.1\ (\mathrm{GeV}/c)^2$ and $n = 6$.

The w functions are given by

$$w_{\mathrm{P}}(\omega') = A_{\mathrm{P}} + B_{\mathrm{P}}\omega' + C_{\mathrm{P}}(1-\omega')^{\frac{1}{2}} ,$$
$$w_{\mathrm{P}'}(\omega') = A_{\mathrm{P}'} + B_{\mathrm{P}'}\omega' + C_{\mathrm{P}'}(1-\omega')^{\frac{1}{2}} , \tag{2.20}$$

and, to ensure analyticity in s, the constants satisfy the conditions

$$\begin{aligned} &A_i > 0 , \quad B_i < 0 , \quad C_i > 0 , \\ &0 \leqslant C_i^2 + 4B_i(A_i+B_i) \leqslant C_i^2 . \end{aligned} \qquad (i = \mathrm{P}, \mathrm{P}') , \tag{2.21}$$

As in ref. [6], we take $B_{\mathrm{P}} = B_{\mathrm{P}'} = -1$, although the values of $A_{\mathrm{P}}, A_{\mathrm{P}'}, C_{\mathrm{P}}$ and $C_{\mathrm{P}'}$ may differ from the nucleon scattering case. For the t-dependent w function, we require for simplicity that $w_\rho(0) = 1$.

The pomeron and P′ trajectories are the same as in ref. [6]; in particular, $\alpha_{\mathrm{P}}(0) = 1$ and $\alpha_{\mathrm{P}'}(0) = \frac{1}{2}$. The t-channel residue functions are real-analytic functions of t, similar to those in the γN scattering case. For the s-channel residue, we adopt the form

$$\gamma^{ii}(\omega') = \frac{k\gamma_{\mathrm{P}'}^{ii} \exp(-g(\omega'))}{\Gamma(n-\alpha_\rho(s))\,[1+(s_t-s)^{\frac{1}{2}}/\Lambda]^m} , \tag{2.22}$$

where k, Λ, n, m are constants. Also, $g(\omega')$ is a real analytic function:

$$g(\omega') = \frac{g_1(2-\omega') + g_2(2-\omega')^2}{[1+((1-\omega')/\Delta)^{\frac{1}{2}}]^4} , \tag{2.23}$$

where g_1, g_2 and Δ are constants. Moreover,

$$\omega' = 1 + \frac{s-s_t}{[a+(s_t-q_1^2)^{\frac{1}{2}}]\,[a+(s_t-q_2^2)^{\frac{1}{2}}]} . \tag{2.24}$$

The function $\gamma^{ii}(s, q_1^2, q_2^2)$ is analytic in the physical s, q_1^2 and q_2^2 sheets, except for normal-threshold cuts. In the limit $s \to \infty$, we have

$$\gamma^{ii}(s, q_1^2, q_2^2) = \mathrm{O}(s^{-\frac{1}{2}m}) , \tag{2.25}$$

where m, Λ and Δ are chosen large and positive.

From (2.13) and (2.22) we find that for large s:

$$\frac{\Gamma(1-\alpha_\rho(s))}{\Gamma(n-\alpha_\rho(s))} \approx (-s)^{1-n} , \tag{2.26}$$

and we see from (2.25) that the direct channel resonance terms ultimately vanish for $s \to \infty$, because $\alpha(\pm\infty) = -\text{const.}$ (this will happen at very large s values).

In the kinematic region where the direct channel resonance terms may be neglected, the structure functions for inelastic electroproduction off pions are given by

$$\nu W_2^\pi(\nu, q^2) = \nu W_2^{\mathrm{P}}(\nu, q^2) + \nu W_2^{\mathrm{P}'}(\nu, q^2)\,, \tag{2.27}$$

where we have included only the dominant P and P′ exchanges, and

$$\nu W_2^{\mathrm{P}}(\nu, q^2) = \frac{-q^2\nu}{\pi}\,\mathcal{F}(q^2, q^2)\,[\gamma_{\mathrm{P}}^{33}[D_3(q^2)]^2 + \tfrac{1}{3}\gamma_{\mathrm{P}}^{88}[D_8(q^2)]^2]$$

$$\times\ \{\tfrac{1}{2}\ln(\omega')\sin\phi_{\mathrm{P}}(\omega') - \tan^{-1}[(\omega'-1)^{\frac{1}{2}}]\cos\phi_{\mathrm{P}}(\omega')\}\,|w_{\mathrm{P}}(\omega')|^{-1}\,, \tag{2.28}$$

$$\nu W_2^{\mathrm{P}'}(\nu, q^2) = \frac{q^2\nu\Gamma(\frac{3}{2})}{\pi}\,\mathcal{F}(q^2, q^2)\,[\tfrac{1}{2}\gamma_{\mathrm{P}'}^{33}[D_3(q^2)]^2$$

$$+ \tfrac{1}{3}\gamma_{\mathrm{P}'}^{88}[D_8(q^2)]^2]\sin(\tfrac{3}{2}\phi_{\mathrm{P}'}(\omega'))\,|w_{\mathrm{P}'}(\omega')|^{-\frac{3}{2}}\,. \tag{2.29}$$

Here, we have neglected the satellite terms in (2.13) and defined $\nu \equiv (s-u)/4m_\pi$, and

$$\phi_i(\omega') = \tan^{-1}\left(\frac{C_i(\omega'-1)^{\frac{1}{2}}}{A_i + B_i\omega'}\right), \qquad (i = \mathrm{P}, \mathrm{P}')\,. \tag{2.30}$$

In the scale invariance limit $-q^2 \to \infty$, $\omega \equiv -2m_\pi\nu/q^2$ fixed, we have

$$\nu W_2^\pi(\nu, q^2) \to F_2^\pi(\omega) = F_2^{\mathrm{P}}(\omega) + F_2^{\mathrm{P}'}(\omega)\,, \tag{2.31}$$

where

$$F_2^{\mathrm{P}}(\omega) = \gamma_{\mathrm{P}}\omega\,\{\tfrac{1}{2}\ln(\omega)\sin\phi_{\mathrm{P}}(\omega) - \tan^{-1}[(\omega-1)^{\frac{1}{2}}]\cos\phi_{\mathrm{P}}(\omega)\}\,|w_{\mathrm{P}}(\omega)|^{-1}\,, \tag{2.32}$$

$$F_2^{\mathrm{P}'}(\omega) = -\gamma_{\mathrm{P}'}\,\omega\,\sin(\tfrac{3}{2}\phi_{\mathrm{P}'}(\omega))\,|w_{\mathrm{P}'}(\omega)|^{-\frac{3}{2}}\,. \tag{2.33}$$

We have defined

$$\gamma_{\mathrm{P}} = \frac{\gamma_{\mathrm{P}}^{33} + \frac{1}{3}\gamma_{\mathrm{P}}^{88}}{2\pi m_\pi}\,, \qquad \gamma_{\mathrm{P}'} = \frac{\Gamma(\frac{3}{2})}{2\pi m_\pi}\,(\tfrac{1}{2}\gamma_{\mathrm{P}'}^{33} + \tfrac{1}{3}\gamma_{\mathrm{P}'}^{88})\,. \tag{2.34}$$

To obtain the structure function W_1^π, we assume that the Callan-Gross relation holds:

$$W_1^{\pi}(\nu, q^2) = (-\nu^2/q^2)\, W_2^{\pi}(\nu, q^2)\,. \tag{2.35}$$

To treat electron-positron annihilation, we write the cross section for $e^+(k) + e^-(k') \to \pi(p)$ + hadrons in terms of the annihilation structure functions $\overline{W}_1^{\pi}$ and $\overline{W}_2^{\pi}$:

$$\frac{d^2\sigma}{d\Omega\, dE_{\pi}} = \left(\frac{2\alpha^2}{q^4}\right)\left(\frac{m_{\pi}^2 \nu}{\sqrt{q^2}}\right)\left(1 - \frac{q^2}{\nu^2}\right)^{\frac{1}{2}}$$
$$\times \left[2\,\overline{W}_1^{\pi}(\nu, q^2) + \frac{2m_{\pi}\nu}{q^2}\left(1 - \frac{q^2}{\nu^2}\right)\frac{\nu \overline{W}_2^{\pi}(\nu, q^2)}{2m_{\pi}} \sin^2\theta\right], \tag{2.36}$$

where $q = k + k'$, $\nu = p \cdot q/m_{\pi}$, θ is the barycentric frame scattering angle and E_{π} is the energy of the detected pion.

Our model has the virtue that, because it is analytic in s, q_1^2 and q_2^2, it may be continued to the annihilation region by using the method described in II:

$$2\pi i \overline{W}_2^{\pi}(\nu, q^2) = T_2^{\pi}(s+i\epsilon, 0, q^2+i\epsilon', q^2-i\epsilon'')$$
$$- T_2^{\pi}(s-i\epsilon, 0, q^2+i\epsilon', q^2-i\epsilon'')\,. \tag{2.37}$$

Here, s is given by

$$s = (-p+q)^2 = m_{\pi}^2 + q^2 - 2m_{\pi}\nu \geqslant m_{\pi}^2\,. \tag{2.38}$$

By evaluating the discontinuity in (2.37), we get

$$\nu \overline{W}_2^{\pi}(\nu, q^2) = \nu \overline{W}_2^{\mathrm{P}}(\nu, q^2) + \nu \overline{W}_2^{\mathrm{P}'}(\nu, q^2) + \overline{R}(\nu, q^2)\,, \tag{2.39}$$

where $\nu\overline{W}_2^{\mathrm{P}}$ and $\nu\overline{W}_2^{\mathrm{P}'}$ are given by the right-hand sides of (2.28) and (2.29), respectively, and $\overline{R}$ is the contribution from the direct channel resonance term in (2.13). It is understood that, in (2.37), q_1^2 and q_2^2 are continued above and below their respective cuts, so that in (2.39) [6]:

$$\omega' = 1 + \frac{s - s_t}{a^2 + q^2 - q_t^2}\,, \tag{2.40}$$

$$\mathcal{F}(q^2, q^2) = 1 + \frac{c^2 q^4 (m_{\omega}^2 - q^2)^2}{(a^2 + q^2 - q_t^2)^6}\,. \tag{2.41}$$

$$[D_3(q^2)]^2 = [(q^2 - m_\rho^2)^2 + \Gamma_3^2(q^2 - 4m_\pi^2)]^{-1} \, . \tag{2.42}$$

The resonance term $\bar{R}$ is given by

$$\bar{R}(\nu, q^2) = \frac{q^2\nu}{\pi} \, \mathrm{Im}\, \{(\tfrac{1}{2}\gamma^{33}(\omega')\,[D_3(q^2)]^2$$

$$+ \tfrac{1}{3}\gamma^{88}(\omega')\,[D_8(q^2)]^2)\Gamma(1 - \alpha_\rho(s))\} \, . \tag{2.43}$$

In evaluating the residue function in (2.43), we use

$$\omega' = 1 + \frac{s - s_t}{a^2 + q^2 - s_t} \tag{2.44}$$

in the annihilation region.

The scaling variable ω for annihilation is defined by

$$\omega = \frac{2m_\pi \nu}{q^2} = 1 + \frac{m_\pi^2 - s}{q^2} \, . \tag{2.45}$$

In the scale invariance limit $q^2 \to \infty$, ω fixed, we get

$$\nu \bar{W}_2^\pi(\nu, q^2) \to \bar{F}_2^\pi(\omega) = \left(\frac{-\omega}{2 - \omega}\right) F_2^\pi(2 - \omega) \, , \tag{2.46}$$

where F_2^π is given by (2.31). We have used (2.25) to neglect the resonance term $\bar{R}(\nu, q^2)$ in the scale invariance limit $s \to \infty$.

According to the Callan-Gross relation (2.35), we have

$$\bar{W}_1^\pi(\nu, q^2) = \frac{-\nu^2}{q^2} \, \bar{W}_2^\pi(\nu, q^2) \, , \tag{2.47}$$

and

$$\bar{F}_1^\pi(\omega) = -\omega \bar{F}_2^\pi(\omega) \, . \tag{2.48}$$

3. Factorization and the pion form factor

Factorization of the Regge residues provides a constraint on the pion structure functions in the Regge region [8] *. We assume that the pomeron and P′ residues

* It should be noted that if we perform a Mellin transform of the pomeron amplitude term in (2.12) then, due to the logarithmic factor, the leading singularity in the angular momentum plane will be a dipole $\approx 1/(J - \alpha(t))^2$, so that factorization of the pomeron is not strictly valid. But we shall assume, nevertheless, that we can factorize the pomeron residue.

for Compton scattering factorize for all values of q^2 in the limit $s \to \infty$. Defining the transverse photoabsorption cross section by

$$\sigma_T(s, q^2) = \frac{4\pi^2 \alpha W_1^\pi(\nu, q^2)}{\nu + q^2/2m_\pi}, \tag{3.1}$$

we obtain for the pomeron contribution in the Regge limit,

$$\sigma_T^P(s, q^2)_\pi = \beta_P^\pi(q^2). \tag{3.2}$$

Here, $\beta_P^\pi(q^2)$ is given by

$$\beta_P^\pi(q^2) = \frac{\pi^2\alpha}{m_\pi} (|B_P| x_1 x_2)^{-1} \mathcal{F}(q^2, q^2)$$

$$\times \{\gamma_P^{33} [D_3(q^2)]^2 + \tfrac{1}{3}\gamma_P^{88} [D_8(q^2)]^2\}. \tag{3.3}$$

In the γp scattering case a similar result is obtained,

$$\sigma_T^P(s, q^2)_p = \beta_P^p(q^2), \tag{3.4}$$

except that m_π is replaced by the nucleon mass M and γ_P^{33} and γ_P^{88} are the residues for nucleon Compton scattering. Factorization means that [8]

$$\beta_P^\pi(q^2) = \frac{\beta_P^p(q^2)\beta_P(\pi N)}{\beta_P(NN)}, \tag{3.5}$$

where $\beta_P(\pi N)$ and $\beta_P(NN)$ are the pomeron residues for πN and NN scattering, respectively. Therefore, we have from (3.3):

$$\gamma_P^{ii}(\gamma\pi) = \gamma_P^{ii}(\gamma p)\left(\frac{m_\pi}{M}\right)\frac{\beta_P(\pi N)}{\beta_P(NN)}, \qquad (i = 3, 8). \tag{3.6}$$

Similarly, we get for the P′ contribution

$$\begin{aligned} \tfrac{1}{2}\gamma_{P'}^{33}(\gamma\pi) &= [\tfrac{1}{3}\gamma_{1\rho}^{33}(\gamma p) + \tfrac{2}{3}\gamma_{2\rho}^{33}(\gamma p)]\left(\frac{m_\pi}{M}\right)\frac{\beta_{P'}(\pi N)}{\beta_{P'}(NN)}, \\ \gamma_{P'}^{88}(\gamma\pi) &= \gamma_\rho^{88}(\gamma p)\left(\frac{m_\pi}{M}\right)\frac{\beta_{P'}(\pi N)}{\beta_{P'}(NN)}. \end{aligned} \tag{3.7}$$

The nucleon Compton residues are given in I as [6]:

$$\gamma_P^{33}(\gamma p) = 0.883 \text{ GeV},$$

$$\gamma_P^{88}(\gamma p) = 0.357 \text{ GeV},$$

$$\gamma_{1\rho}^{33}(\gamma p) + 2\gamma_{2\rho}^{33}(\gamma p) = 5.12 \text{ GeV},$$

$$\gamma_\rho^{88}(\gamma p) = 0.669 \text{ GeV}, \tag{3.8}$$

and the residues $\beta_{P,P'}(\pi N)$ and $\beta_{P,P'}(NN)$ read [8, 10]

$$\beta_P(\pi N) = 20.1 \text{ mb}, \qquad \beta_{P'}(\pi N) = 19.8 \text{ mb},$$

$$\beta_P(NN) = 35.6 \text{ mb}, \qquad \beta_{P'}(NN) = 44.3 \text{ mb}. \tag{3.9}$$

Therefore, our pion Compton residues are determined to be

$$\gamma_P^{33} = 0.074 \text{ GeV}, \qquad \gamma_{P'}^{33} = 0.228 \text{ GeV},$$

$$\gamma_P^{88} = 0.030 \text{ GeV}, \qquad \gamma_{P'}^{88} = 0.045 \text{ GeV}, \tag{3.10}$$

and the residues γ_P and $\gamma_{P'}$, defined in (2.34), have the values

$$\gamma_P = 0.096, \qquad \gamma_{P'} = 0.13. \tag{3.11}$$

The scale-invariant structure function F_2^π defined in (2.31) is now determined, except for the parameters A_P, C_P, $A_{P'}$ and $C_{P'}$, which control the threshold behaviour of the structure function for $\omega \to 1$. We have found that $F_2^\pi(\omega)$ has smooth threshold behaviour if

$$A_P = 1.0001, \qquad A_{P'} = 1.94,$$

$$C_P = 0.52, \qquad C_{P'} = 1.94. \tag{3.12}$$

This is shown in fig. 1, where we plot $F_2^\pi(\omega)$ *versus* ω.

Having obtained the scale-invariant structure function, we may use the Bloom-Gilman sum rule [7, 8]

$$[F_\pi(q^2)]^2 = \int_1^{1+(W_\pi^2 - m_\pi^2)/(-q^2)} F_2^\pi(\omega)\,\mathrm{d}\omega, \tag{3.13}$$

to predict the pion form factor $F_\pi(q^2)$. There is some freedom in the choice of the upper limit for the integration in (3.13), although it should not include too much contribution from the higher resonances. With the value $W_\pi^2 = 1.7 \text{ GeV}^2$, we obtain

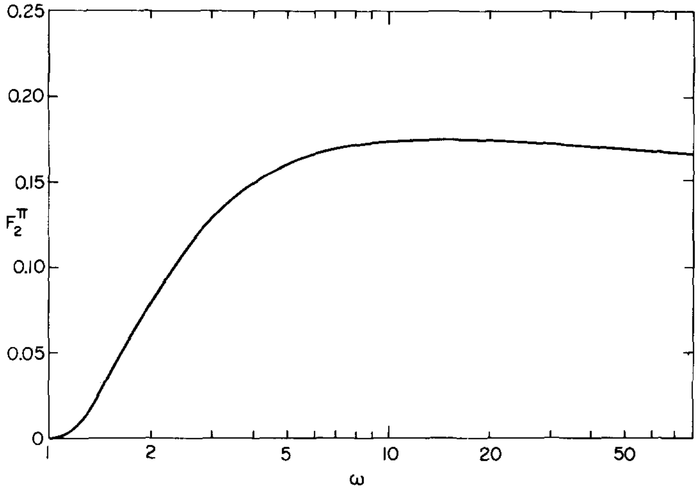

Fig. 1. The scale-invariant structure function F_2^π for electroproduction is plotted *versus* ω.

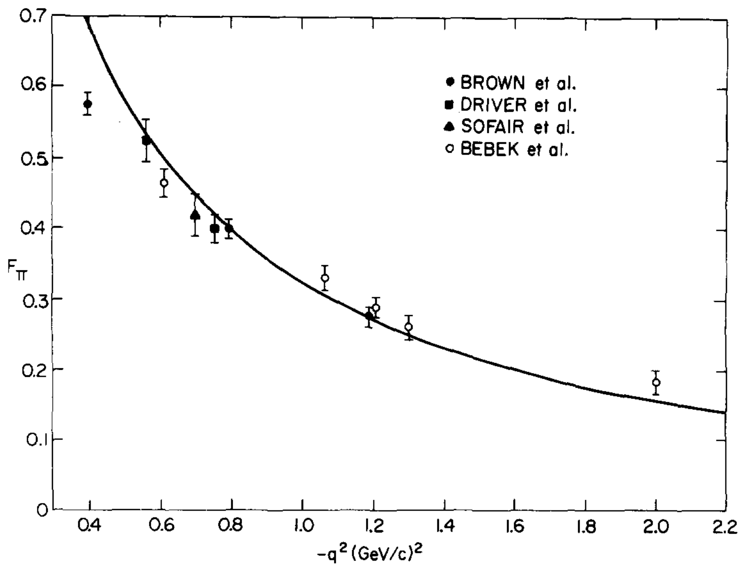

Fig. 2. The pion form factor $F_\pi(q^2)$, obtained from the Bloom-Gilman sum rule, is shown as a solid line. The data are taken from ref. [11].

the prediction for the pion form factor shown in fig. 2 along with recent data *. Since (3.13) is not expected to be valid as $-q^2 \to 0$ (in fact, it diverges as $-q^2 \to 0$ in our model), we show our prediction for $-q^2 \gtrsim 0.4\ (\mathrm{GeV}/c)^2$. Our model reproduces well both the magnitude and shape of the pion form factor, which lends support to our use of factorization to obtain the scale-invariant pion structure function.

4. A sum rule for the multiplicity

In the annihilation region, our model deals with the one-particle inclusive process $e^+ + e^- \to \pi$ + hadrons in the one-photon-exchange approximation. To treat the totally inclusive process $e^+ + e^- \to$ hadrons, we make use of two inclusive sum rules

$$\iint \frac{d^2\sigma}{d\Omega\, dE}\, d\Omega\, dE = \langle n_\pi \rangle\, \sigma_{tot}(q^2)\,, \tag{4.1}$$

and

$$\sum_c \iint \frac{d^2\sigma^c}{d\Omega\, dE_c}\, E_c\, d\Omega\, dE_c = \sqrt{q^2}\, \sigma_{tot}(q^2)\,. \tag{4.2}$$

In (4.1), $\langle n_\pi \rangle$ is the mean multiplicity of the given pion. The sum rule (4.2) is a consequence of energy conservation, and the sum is over all species of hadrons which could be produced in electron-positron collisions. We expect that production of kaons, nucleons, etc., should amount to less than 10% of the production of pions, so that we may restrict the sum in (4.2) to pions. Furthermore, in our model the π^+, π^- and π^0 production cross sections are equal, so that (4.2) may be written

$$3\iint \frac{d^2\sigma}{d\Omega\, dE}\, E\, d\Omega\, dE = \sqrt{q^2}\, \sigma_{tot}(q^2)\,. \tag{4.3}$$

The mean multiplicity is then obtained by combining (4.1) and (4.3):

$$\langle n_\pi \rangle = \frac{\sqrt{q^2} \iint \dfrac{d^2\sigma}{d\Omega\, dE}\, d\Omega\, dE}{3\iint \dfrac{d^2\sigma}{d\Omega\, dE}\, E\, d\Omega\, dE}\,. \tag{4.4}$$

In the scale-invariant limit $q^2 \to \infty$, we get

$$\langle n_\pi \rangle = \frac{2}{3}\, \frac{\displaystyle\int_{2m_\pi/\sqrt{q^2}}^{1} \omega \bar{F}_1(\omega)\, d\omega}{\displaystyle\int_{2m_\pi/\sqrt{q^2}}^{1} \omega^2 \bar{F}_1(\omega)\, d\omega}\,. \tag{4.5}$$

* The data are taken from the review article by Berkelman [11].

5. Results for e$^+$e$^-$ annihilation

The recent experimental results obtained by the SLAC-LBL-SPEAR group [2], have certain remarkable features. The inclusive differential cross section $E_\pi d^3\sigma/d^3p_\pi$ is similar to an analogous distribution for pp $\rightarrow \pi$X at 90° observed at NAL [12] *. Measurements of $\sigma(e^+e^- \rightarrow \text{hadrons})$ in the range 16 to 25 GeV^2, which have been made at CEA and SLAC, are consistent with a constant or slowly falling cross section in this range of q^2. Moreover, the ratio $R = \sigma(e^+e^- \rightarrow \text{hadrons})/\sigma(e^+e^- \rightarrow \mu^+\mu^-)$ conflicts with the predictions of the parton model, current algebra and asymptotically free non-Abelian gauge theories.

It has been suggested [13] that there may exist a lepton-hadron interaction which produces these unexpected results, but such a suggestion may conflict with quantum electrodynamics.

We shall explain the SLAC results in our model by observing that the missing mass channel resonances (ρ, ω, ϕ, etc. . .) build up in a "statistical bootstrap" way to give a diffractive-type of scattering similar to that found in hadronic pp collisions. The mechanism for this is already contained in our model in the term $\bar{R}(\nu, q^2)$, in eqs. (2.39) and (2.43), which was taken to be negligible in our previous work [6] on e$^+$ + e$^-$ $\rightarrow \bar{\text{p}}$ + X, due to the meagre production of baryon resonances in the missing mass channel (this latter assumption is, of course, subject to experimental verification).

To treat σ_{tot} and $\langle n_\pi \rangle$, we employ the sum rules (4.1) and (4.3). From the Callan-Gross relation (2.47), we see that the inclusive cross section (2.36) depends only on $\nu\bar{W}_2(\nu, q^2)$. Our model for $\nu\bar{W}_2(\nu, q^2)$ is given by (2.39), with $\nu\bar{W}_2^{\text{P}}$, $\nu\bar{W}_2^{\text{P}'}$ and $\bar{R}$ given by (2.28), (2.29) and (2.43), respectively. The terms $\nu\bar{W}_2^{\text{P}}$ and $\nu\bar{W}_2^{\text{P}'}$ have been fixed by the discussion of sect. 3, so that only $\bar{R}$ may be varied to fit σ_{tot} and $\langle n_\pi \rangle$.

We choose Λ and Δ large, so that the factor involving Λ and m in (2.22) may be replaced by 1 at moderate values of s. Then $\bar{R}$ is fixed by choosing values for n, k, g_1 and g_2 in (2.22) and (2.23). The parameter k sets the normalization of the cross section, n controls the energy dependence of the cross section through (2.26), and g_1 and g_2 are important for the ω-dependence of $\nu\bar{W}_2$, and hence, *via* (4.4), for the multiplicity. Only by simultaneously fitting both σ_{tot} and $\langle n_\pi \rangle$ can n, k, g_1 and g_2 all be determined.

By choosing $n = \frac{1}{2}$, $k = 1.68 \times 10^6$, $g_1 = 13.0$ and $g_2 = 0.1$, we obtain $\sigma(e^+e^- \rightarrow \text{hadrons})$ shown in fig. 3 and compare it with the world's data [14]. In fig. 4 we compare our result for $R = \sigma(e^+e^- \rightarrow \text{hadrons})/\sigma(e^+e^- \rightarrow \mu^+\mu^-)$ with the CEA and Frascati data. Since $\omega' \rightarrow \omega$ in the scale invariance limit, we see that scale invariance of $\bar{R}$ is broken by the factor involving Λ and m in (2.22), and by the factor $\sqrt{q^2}$ coming from (2.26) when $n = \frac{1}{2}$. Hence, the ratio R will rise linearly *versus* $\sqrt{q^2}$ until q^2 is of the order of either Λ or $\Delta\rho$ (the parameter which determines the asymptotic regime of the ρ trajectory [6]), whichever is smaller. Since m is large $\bar{R}$ will

* Note that at 90°, p and $p_\perp$ are equal.

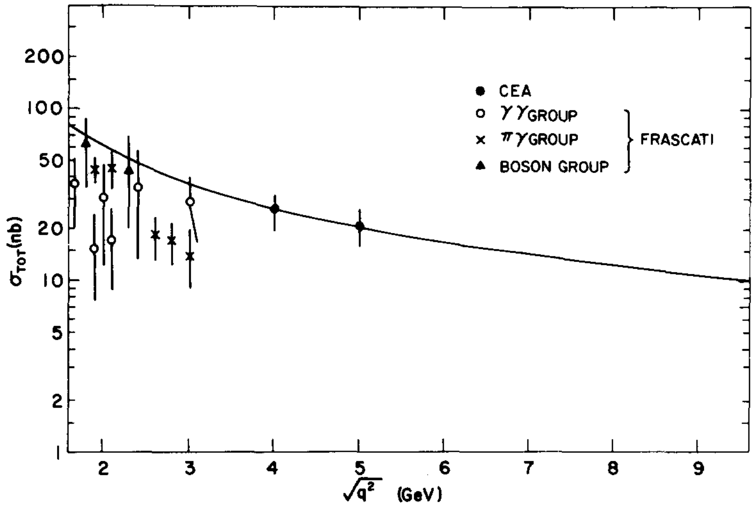

Fig. 3. Our fit to the cross section $\sigma(e^+e^- \to \text{hadrons})$ (solid line) as a function of $\sqrt{q^2}$ is compared with the world's data, quoted in ref. [14].

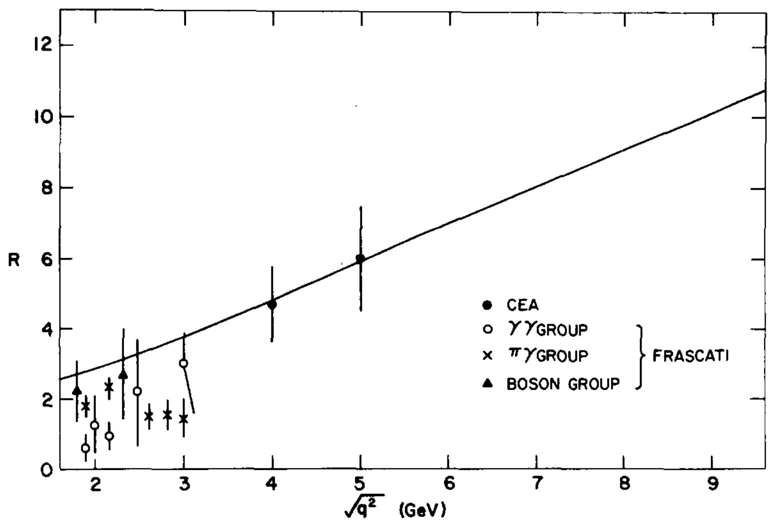

Fig. 4. The resulting ratio $R = \sigma(e^+e^- \to \text{hadrons})/\sigma(e^+e^- \to \mu^+\mu^-)$ is displayed as a solid line against the data. Note the linear increase in $\sqrt{q^2}$.

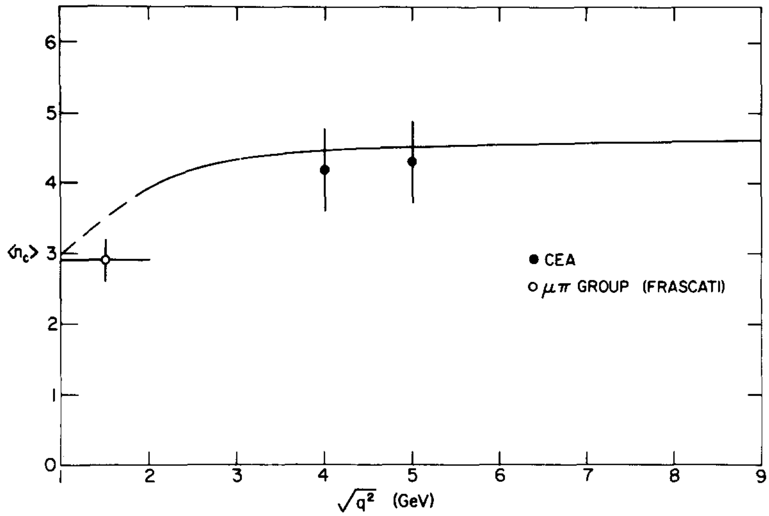

Fig. 5. Our fit to the multiplicity $\langle n_c \rangle$ for the production of charged pions, plotted against $\sqrt{q^2}$ and compared with the data (refs. [1, 15]).

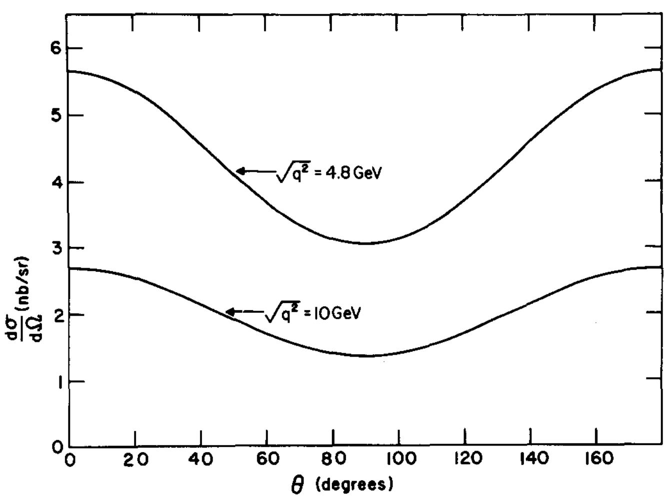

Fig. 6. The predicted angular distribution $d\sigma/d\Omega$ *versus* θ for $\sqrt{q^2} = 4.8$ and 10 GeV.

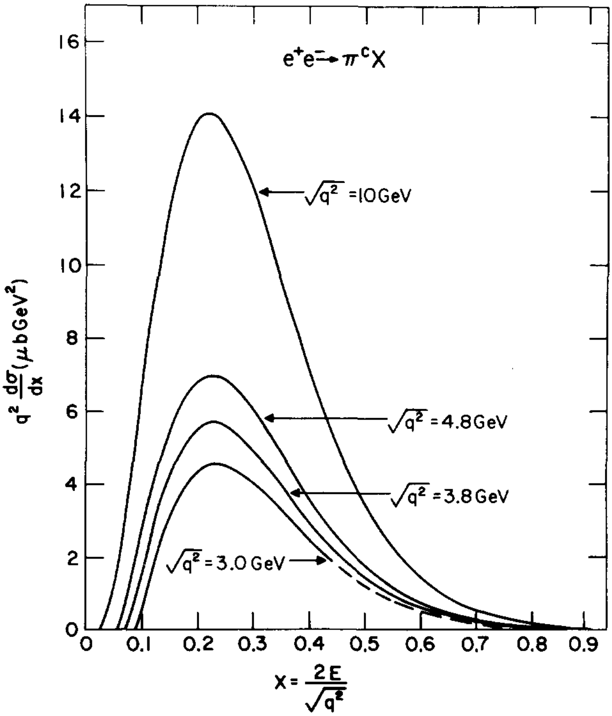

Fig. 7. The predicted $q^2 d\sigma/dx$ for $e^+e^- \to \pi^c$ + hadrons plotted *versus* $x = 2E/\sqrt{q^2}$ for $\sqrt{q^2}$ = 3.0, 3.8, 4.8 and 10 GeV, and showing a marked breaking of scaling for $x \leqslant 0.5$. The dashed part of the curve for $\sqrt{q^2}$ = 3.0 GeV corresponds to $s < 5$ GeV^2.

vanish as $q^2 \to \infty$, and R will eventually tend to the value 1.45×10^{-3}, given by the scale-invariant P and P$'$ terms. The P and P$'$ terms become scale-invariant at relatively low values of q^2; for example, at $q^2 = 25$ GeV^2 they contribute 0.03% to $R = 5.89$.

Our fit to the multiplicity $\langle n_c \rangle$ for the production of charged pions is shown in fig. 5 and compared with CEA and Frascati data [1, 15]. The multiplicity is predicted to rise slowly *versus* $\sqrt{q^2}$ and then tend to the value 2.26 given by (4.5) as $\sqrt{q^2} \to \infty$. We observe from eq. (4.4) that this prediction depends only on the shape of the structure functions. We also note that the asymptotic values $\langle n_c \rangle = 2.26$ and $R = 1.45 \times 10^{-3}$ constitute *predictions* determined by the discussion of sect. 3, and completely independent of the form $\bar{R}$.

Having fixed the parameters in our model, we can now examine the inclusive cross section. In fig. 6, we display the predicted angular distribution $d\sigma/d\Omega$ and we see that it is fairly flat between 45° and 135°. By integrating the cross section $q^2 d^2\sigma^\pi/d\Omega\, dx$ for the inclusive reaction $e^+e^- \to \pi^- X$ over all angles we obtain the

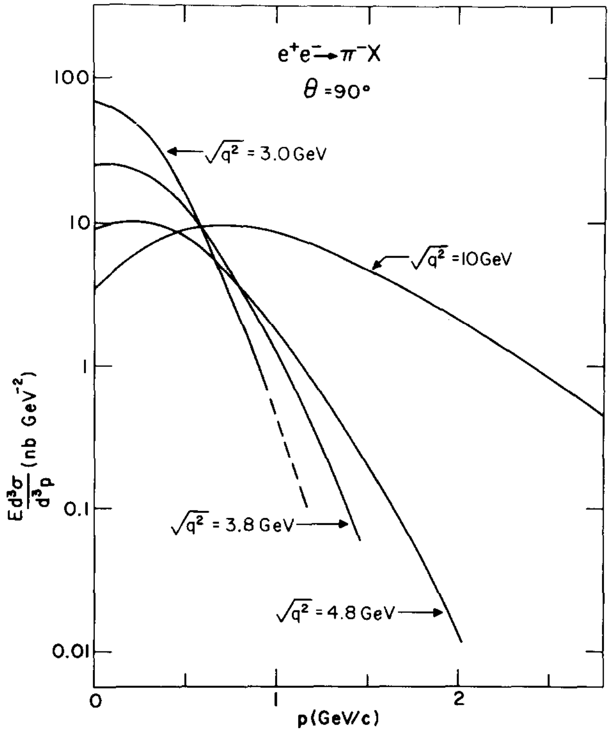

Fig. 8. Our prediction for $E\,\mathrm{d}^3\sigma/\mathrm{d}p^3$ at 90° for $e^+e^- \to \pi^-$ + hadrons, plotted on a logarithmic scale *versus* p at $\sqrt{q^2}$ = 3.0, 3.8, 4.8 and 10 GeV.

predictions shown in fig. 7, plotted *versus* $x = 2E/\sqrt{q^2}$ for $\sqrt{q^2}$ = 3.0, 3.8, 4.8 and 10 GeV. We see that there is a marked breaking of scaling in fig. 7 for $x \leqslant 0.5$.

In fig. 8, we show our results for $E_\pi\, \mathrm{d}^3\sigma/\mathrm{d}p^3$. The predicted slope is approximately the same at 90° as in the process $pp \to \pi^- X$ measured at NAL [12] when $\sqrt{q^2}$ = 4.8 GeV.

Finally, in fig. 9, we display the predicted annihilation structure function $2m_\pi \overline{W}_1^\pi$, plotted *versus* ω for $\sqrt{q^2}$ = 4.8 and 10 GeV. Again we observe the strong scale-breaking effects around $\omega \sim 0.2$.

It should be mentioned at this point that we do not expect our small q^2 predictions to be accurate, because we have not, as yet, treated the resonance pole contributions correctly for $q^2 \lesssim 5$ GeV^2.

If the QED inequality [9]

$$\frac{\alpha}{3\pi}\int \frac{R(q^2)}{q^2}\,\mathrm{d}q^2 < 1 \tag{5.1}$$

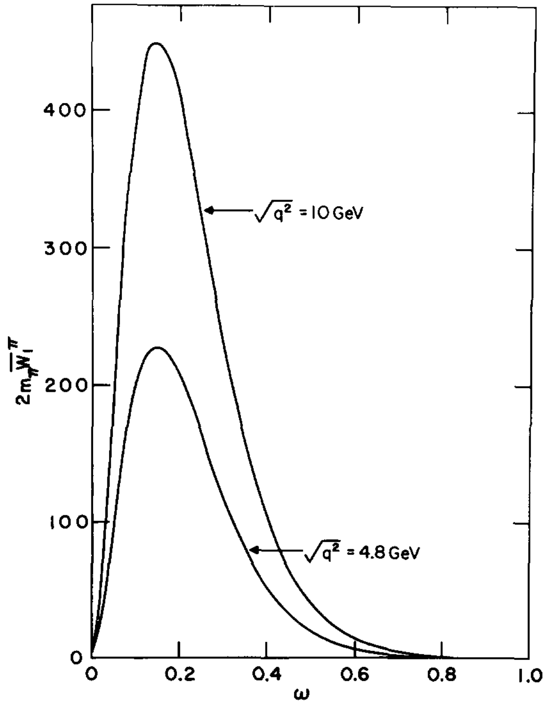

Fig. 9. Predicted annihilation structure function $2m_\pi \overline{W}_1$ plotted *versus* ω for $\sqrt{q^2}$ = 4.8 and 10 GeV. Note the strong scale-breaking around ω = 0.2.

is to hold, we find that the behaviour of R predicted in fig. 4 may continue up to $\sqrt{q^2} \approx 550$ GeV. As discussed above, the extent to which this behaviour may continue is controlled by the parameters Λ and $\Delta\rho$, and without a knowledge of their values we cannot say whether the bound (5.1) is satisfied or violated in our model.

It is important to recognize that all our results are based on the one-photon exchange approximation.

6. Discussion of results

From our unified description of current-hadronic processes in I and II and in the present work, we have succeeded in fitting a remarkable amount of data. Our results for $e^+e^- \to \pi X$ are consistent with the CEA-SLAC data and have their origin in a simple physical mechanism, namely, the build-up of resonances in the multi-pion missing mass channel. One can only expect to get detailed predictions, as we have obtained, from a model which contains a great deal of information about the dynamics of the interactions; such a model can be found by using S-matrix methods based on well-founded physical properties, such as analyticity, crossing symmetry, Regge behaviour, vector-meson dominance, etc. It is too early to say what connection, if any, a physical description of this kind has with the constituent picture of the hadrons.

We thank Dr. I.O. Moen for a helpful and stimulating discussion.

References

[1] A. Litke et al., Phys. Rev. Letters 30 (1973) 1189;
G. Tarnopolsky et al., Phys. Rev. Letters 32 (1974) 432.
[2] B. Richter, Results obtained by the SLAC-LBL-SPEAR collaboration reported at the Chicago meeting, 1974.
[3] A. Bramon, E. Etim and M. Greco, Phys. Letters 41B (1972) 609;
M. Greco, Nucl. Phys. B63 (1973) 398;
J.J. Sakurai, Phys. Letters 46B (1973) 207.
[4] R.P. Feynman, Phys. Rev. Letters 23 (1969) 1415;
S.D. Drell, D.J. Levy and T.M. Yan, Phys. Rev. Letters 22 (1969) 744;
J.D. Bjorken and E. Paschos, Phys. Rev. 185 (1969) 1975;
P. Landshoff and J.C. Polkinghorne, Nucl. Phys. B28 (1971) 240;
J. Kuti and V.F. Weisskopf, Phys. Rev. D4 (1971) 3418.
[5] G. West, Stanford preprint (1974).
[6] J.W. Moffat and A.C.D. Wright, Phys. Rev. D8 (1973) 2152; University of Toronto preprint (1974). These are referred to as I and II in the text, respectively.
[7] E.D. Bloom and F.J. Gilman, Phys. Rev. Letters 25 (1970) 1140.
[8] J.W. Moffat and V.G. Snell, Phys. Rev. D4 (1971) 1452.
[9] J.D. Bjorken and B.L. Ioffe, SLAC-PUB-1467 (1974).
[10] V. Barger, M. Olsson and D. Reeder, Nucl. Phys. B5 (1968) 411.
[11] K. Berkelman, Proc. 1971 Int. Symposium on electron and photon interactions at high energies, ed. N.B. Mistry (Laboratory of Nuclear Studies, Cornell University, Ithaca, New York, 1972);
C.J. Bebek et al., Phys. Rev., to be published.
[12] J.W. Cronin et al., Phys. Rev. Letters 31 (1973) 1426.
[13] O.W. Greenberg and G.B. Yodh, University of Maryland report No. 74-062 (1974);
J.C. Pati and A. Salam, University of Maryland report No. 74-069 (1974).
[14] K. Strauch, Rapporteur talk in Proc. of the Int. Symposium on electron and photon interaction at high energies, Bonn, Germany, 1973 (North-Holland, Amsterdam, 1974).
[15] F. Ceradini et al., Contributed paper to the Int. Symposium on electron and photon interactions at high energies, Bonn, 1973.